Research Article | Vol. 1, No. 4 | 15 Dec 2018 | OSA CONTINUUM 1260

OSA CONTINUUM

Using silica fiber coupling to extend superconducting nanowire single-photon detectors into the infrared

PAULINA S. KUO*

Information Technology Laboratory, National Institute of Standards and Technology, 100 Bureau Drive, Gaithersburg, Maryland 20899, USA
*paulina.kuo@nist.gov

Abstract: There is growing interest in superconducting nanowire single-photon detectors (SNSPDs) for their high detection efficiency, low noise, and broad wavelength-sensitivity range. Typically, silica fibers are used to deliver light to the detectors inside the cryostat, which works well for wavelengths from visible through 1550 nm. To access longer-wavelength infrared photons, other types of fibers, such as chalcogenide and fluoride fibers, need to be used. Here, we examine the infrared-wavelength transmission of straight and coiled silica optical fibers as candidates to couple infrared light to SNSPDs. We find that the silica fibers offer good transmission up to 2.2 μm wavelength. Above this wavelength, the transmission rolls off; the fibers exhibit 3 dB/m loss at 2.5 μm. High bend-loss sensitivity of some fibers can be used to adjust the long-wavelength transmission cutoff of the fiber to limit noise photons due to blackbody radiation.

Superconducting nanowire single-photon detectors (SNSPDs) have become increasingly attractive detectors because of their high detection efficiency, low background noise and low timing jitter [1]. System detection efficiencies up to 93% with less than 1 count per second intrinsic detector dark count rate have been shown at 1550 nm [2]. In contrast with semiconductor detectors that have an associated bandgap, the drop-off in detection efficiency of SNSPDs seems to occur more gradually in wavelength [3, 4]. Reference [4] observed that amorphous WSi SNSPDs show decreasing intrinsic detection efficiency of the SNSPDs as the incident photon wavelength was varied from 2 to 6 μm with associated changes in the bias-current response. Reasonably good intrinsic detection efficiencies can be obtained at 6 μm wavelengths with larger bias currents. Efficient single-photon detection using SNSPDs has been shown up to 5 μm [5], 6 μm [4] and 7 μm wavelengths [6].

The infrared (IR) wavelength range is very attractive for single-photon detection because of applications in sensing and spectroscopy. Unfortunately, IR detection using SNSPDs is challenging because the primary source of noise is blackbody radiation [5–10]. Room temperature (T = 300 K) blackbody radiation is peaked at 9.7 μm with a tail that extends into the near-IR wavelength range. Bandpass filters have been used to reject the noise photons [9, 11, 12]. Tight coiling of the optical fiber that delivers the photons to the SNSPDs can also be used to block the long-wavelength noise photons and reduce extrinsic noise counts [10]. Alternatively, the entire experiment can be cooled to liquid nitrogen temperatures. Using this strategy, Chen et al. [6] showed a 100-fold improvement in signal-to-noise ratio using SNSPDs compared to a conventional liquid-nitrogen-cooled InSb detector.

Silica fibers have long been the workhorse in optical fiber telecommunications, particularly near 1550 nm wavelength. However, significantly less attention has been paid to their performance beyond 1550 nm but before the material absorption edge. This wavelength range is potentially of interest for sensing of carbon dioxide, methane or other molecular species [13]; for silicon photonics [14] and for quantum communications [15]. Silica fibers have advantages over

#345917 https://doi.org/10.1364/OSAC.1.001260
Journal © 2018 Received 14 Sep 2018; accepted 26 Oct 2018; published 30 Nov 2018

OSA CONTINUUM

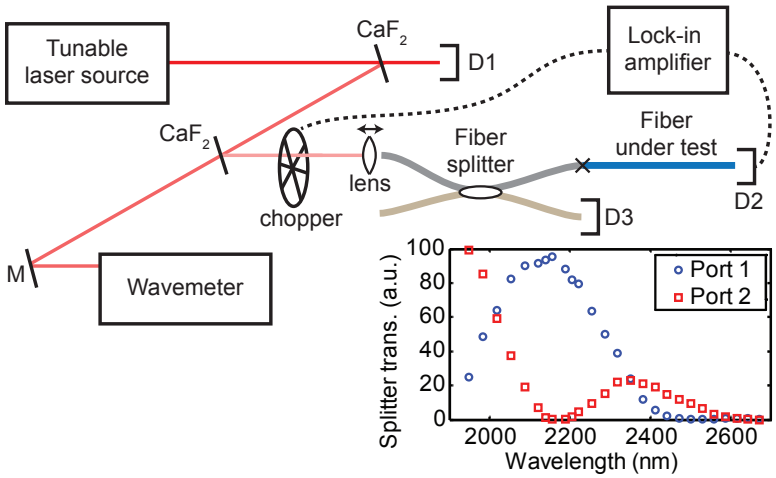

Fig. 1. Diagram of the experimental setup. Reflections from two CaF_2 plates attenuated the laser to milliwatt level. Detectors 1 and 3 (D1 and D3) were thermal power meters used to monitor the power while the transmission through the fiber under test was measured with an InAs detector (D2). The wavelength of the laser was measured with an infrared wavemeter preceded by a silver turning mirror (M). The transmission is measured by comparing the power at D2 with and without the fiber under test. Dashed lines indicate electrical connections. The lower-right inset shows the measured transmission of the fiber splitter.

chalcogenide, fluoride and other infrared fibers in their mechanical robustness and low optical losses. It is useful to determine the longest wavelength that silica fibers may be used before absorption losses become large. In this work, we measure the transmission of two silica optical fibers, SMF-28 and SM2000, between 2000 nm and 2700 nm to observe the absorption edges of the fibers. We also characterize the transmission for different coiling diameters, which is important for filtering undesired background counts due to blackbody radiation.

The transmission data of bulk glass and fused silica are widely available in the literature. The long-wavelength cutoff of silica materials varies by up to 0.5 μm in wavelength depending on processing and dopants [16, 17]. Measurements of silica optical fiber also show variations in transmission [16, 18–20]. Often these papers focused on long-distance fiber transmission at wavelengths below 2 μm with reported losses below 50 dB/km, which corresponds to transmission $> 98.85\%$ in a 1 meter length of fiber. More recently, Smirnov et al. [10] measured the infrared transmission of SMF-28 fiber but only at wavelengths shorter than 1.7 μm. Our measurements present transmission of SMF-28 and SM2000 fibers at wavelengths up to 2.7 μm.

The experimental setup is shown in Fig. 1. A continuous-wave (CW), narrow-linewidth laser source tunable between 1950 nm and 2700 nm (IPG Photonics CLT laser) was attenuated and focused into an optical fiber. The laser produced up to 4.7 W of CW power, which we attenuated down to milliwatt-level using two consecutive reflections from a pair of uncoated CaF_2 plates (3% reflection per face). An infrared wavemeter (Bristol 621B) was used to monitor the wavelength of the laser. Light reflected off the second CaF_2 plate was focused into the input of a fiber splitter using an infrared aspheric lens with 11 mm focal length. The lens was held in a translating mount to adjust the separation distance between the lens and the fiber tip in order to account for chromatic aberration of the lens due to the wide tuning range of the laser. The fiber splitter was made of fused SM2000 fiber and was used to monitor the power coupled into the input fiber. We were unable to find a fiber splitter with a constant split-ratio over the broad 1950 nm to 2700 nm tuning range. The transmission of the fiber splitter is shown in the inset of Fig. 1. The power transmitted through the test fiber was measured using an amplified InAs detector, while two

OSA CONTINUUM

thermal power meters were used to monitor the total power of the laser and the power in the secondary port of the fiber splitter. The laser beam was chopped around 630 Hz (much faster than the response time of the thermal power meters) and the voltage from the InAs detector was read by a lockin amplifier.

The transmission was determined by taking the ratio of power readings with the test fiber and with the test fiber removed. We found that monitoring the power at the secondary port of the fiber splitter was important for insuring repeatability of the measurements as the laser wavelength was scanned, especially as the focusing lens was adjusted at each wavelength step to optimize the power coupled into the fiber. We chose not to normalize the main power reading to the power measured at the secondary port of the fiber splitter because in certain wavelength ranges, the transmission of the secondary port of the fiber splitter was very small (see inset of Fig. 1) and at these wavelengths, the noise of the thermal meter (D3) dominates the reading. We did normalize the transmitted power readings to the total laser power observed by D1 to eliminate power fluctuations of the laser itself.

We measured the infrared transmission of two silica fibers: Corning SMF-28 and ThorLabs SM2000. Figure 2 show results of the transmission measurements. In Fig. 2(a), we compare several lengths of SMF-28 and SM2000 fiber. We measured 1 meter long fibers as well as a 3 meter long SMF-28 fiber and a 5 meter long SM2000 fiber. The measurements indicate that 1 m long SMF-28 and SM2000 fibers have the same transmission. Both fibers exhibit good transmission up to 2200 nm. Above this wavelength, there is a gradual decrease in transmission. 3 dB/m loss is observed in the fibers at about 2.5 μm.

Even though SMF-28 fiber is designed for low-loss operation at the 1550 nm telecommunications wavelength, we observed that the fiber has good transmission to at least 2200 nm. Fused silica and fused quartz materials typically transmit to beyond 2 μm wavelength [17], so it is perhaps not surprising that SMF-28 fiber transmits well to 2200 nm. For coupling to SNSPDs, fibers are several meters in length rather than kilometers and a few percent loss can be tolerated. It is attractive to use silica fiber to extend SNSPD systems to 2200 nm because the fiber is robust and widely available. Beyond 2200 nm, there is higher attenuation; our measurement of 1 m long SMF-28 fiber shows 50% transmission at 2500 nm. For much longer wavelengths, other fiber materials must be used, such as chalcogenide or fluoride fibers [16].

SM2000 fiber is another commercial silica fiber, which is designed for single mode operation between 1.7 and 2.3 μm [21]. The data in Fig. 2(a) indicate that the transmission of uncoiled SM2000 fiber is the same as the transmission for SMF-28 fiber, which seems reasonable since both are silica fibers. However, the fibers behave differently when coiled.

Figures 2(b) and 2(c) plot the transmission of 1 meter long SMF-28 and SM2000 fibers with different coiling diameters. For these measurements, we coiled a 30 cm section of each fiber. Figure 2(b) shows results for SMF-28 fiber while Fig. 2(c) shows results for SM2000 fiber. The data are labeled by the diameter of the fiber coils. As a side note, when probing the fiber under test, there is an additional FC-FC fiber connection compared to when the test fiber is removed. We assumed the extra connection leads to a few percent loss that is independent of wavelength. We disregarded the connector loss by scaling data to obtain transmission of 100% at short wavelengths. The data for the tightest coiling of the two fibers was not scaled.

The data show that SM2000 fiber has less sensitivity to bending than SMF-28 fiber; tighter bends in SM2000 fiber are needed to achieve the same long-wavelength attenuation as in SMF-28 fiber. This lower bend sensitivity in SM2000 fiber is related to its larger core size (11 μm core diameter for SM2000 fiber compared to 8.2 μm diameter for SMF-28 [21, 22]). For SNSPD systems, bending the fiber is useful for managing blackbody radiation that contributes to noise counts. Therefore, the higher bend sensitivity of SMF-28 fiber is attractive because looser coils are needed to obtain the same attenuation of the long-wavelength blackbody radiation. The looser coils have less strain inside the fiber, which may be useful for avoiding material fatigue.

OSA CONTINUUM

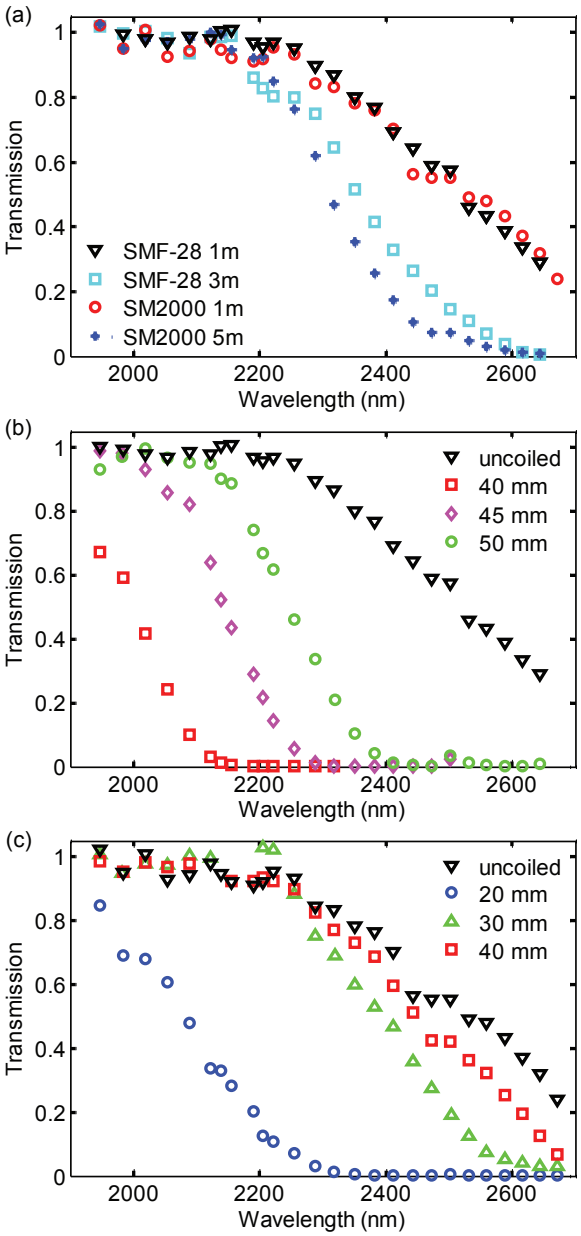

Fig. 2. (a) Transmission of different lengths of SMF-28 and SM2000 fiber. Transmission of (b) 1 m SMF-28 fiber and (c) 1 m SM2000 fiber at different coil diameters. A 30-cm-long section of each fiber was coiled. The SMF-28 fiber is more sensitive to bending, which is reflected by the larger coiling diameters in (b) compared to (c).

OSA CONTINUUM

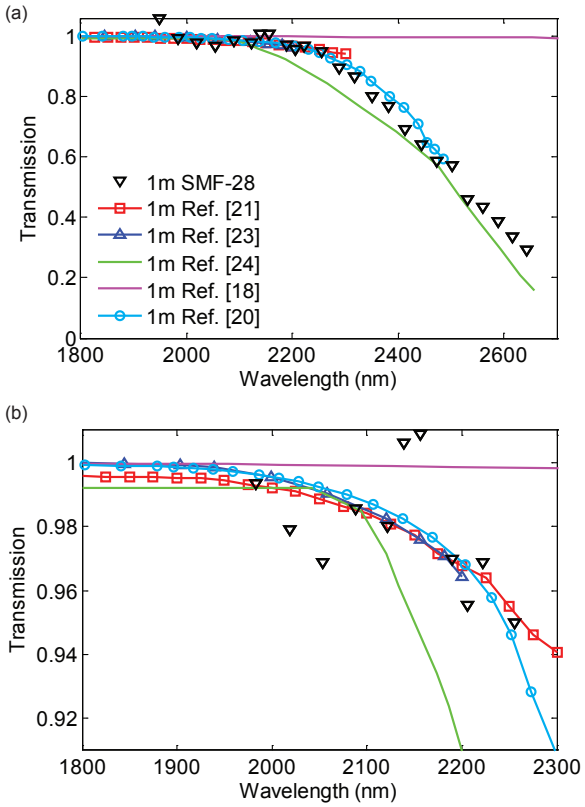

Fig. 3. (a) Comparison of transmission for 1 meter lengths of fiber. We compare our measured transmission for SMF-28 fiber to the transmission calculated from Refs. [18, 20, 21, 23, 24]. The line for Ref. [18] represents an extrapolation of data taken below 2 μm, which is in poor agreement with other measurements. (b) Zoom in of the same transmission data in the region between 1800 nm and 2300 nm.

In Fig. 3, we compare our measured transmission for 1 meter long, uncoiled fiber to the transmission calculated from other references in the literature. Figure 3(b) shows a zoom in of the same data shown in Fig. 3(a). Our measured results are in reasonably good agreement with Refs. [24] (silica fiber) and [20] (GeO_2-SiO_2 step type fiber). Data in Refs. [23] and [21] are for SM2000 fiber, but only extend to 2200 nm and 2300 nm, respectively. It is dangerous to extrapolate to longer wavelengths, which is demonstrated by Ref. [18]. These authors attempt to extrapolate absorption data taken below 2 μm to longer wavelength, which unfortunately do not agree with other measurements in the literature. As seen in Fig. 3, the loss at 2300 nm reported by Ref. [21] is higher than our data and other reports in the literature. Extrapolation of results from [21] to longer wavelengths will likely yield incorrect results.

Our coiled-fiber transmission measurements are mostly consistent with other published measurements. Smirnov et al. [10] report on coiled SMF-28 fiber at bending diameters 21 mm and below. These tightly bent fibers show significant attenuation below 1.8 μm, which is consistent with our observed trends for SMF-28. Ref. [21] reports on bending losses for SMF-28 and SM2000 fibers at 1996 nm with 30 mm coil diameter. Converting the loss values in Ref. [21] to the transmission of a 30-cm-long section of coiled fiber, we calculate 94.7% transmission for SM2000 fiber and 10.9% transmission for SMF-28 fiber, which are consistent with measurements presented in Fig. 2. There is some disagreement between our results and coiling loss for SM2000

OSA CONTINUUM

fiber described in Ref. [21]. For instance, our data show higher attenuation at 2500 nm for the same coiling diameters. It is difficult to speculate on the source of this disagreement. Reference [21] perform measurements on a single loop of fiber while we coiled a 30-cm section of fiber, so the relative uncertainty in coiled-fiber length is higher in Ref. [21] than the measurements presented here. Our data present a clearer picture than previously published data of coiled and uncoiled fiber transmission between 2000 nm and 2700 nm.

In conclusion, we show that SMF-28 and SM2000 fibers can be used with SNSPD systems to delivery photons up to 2200 nm in wavelength. As also described in Ref. [10], coiling the fiber is an effective way to attenuate longer-wavelength photons due to block blackbody radiation, which is the dominant source of noise for SNSPDs. For instance, our measurements show that coiling SMF-28 fiber to 40 mm diameter will produce 20 dB/m attenuation at 2050 nm. Our data can be combined with theoretical models of bent fibers [25–27] to better design filtering to reject blackbody noise photons. Our results present a convenient way to extend superconducting nanowire single-photon detector systems into the infrared wavelength range (to 2200 nm and perhaps even slightly beyond this wavelength) by using silica optical fibers.

Acknowledgment

The author thanks Brian Alberding for assistance with the laser.

Certain commercial equipment or materials are identified in this paper in order to specify the experimental procedure adequately. Such identification is not intended to imply recommendation or endorsement by the National Institute of Standards and Technology, nor is it intended to imply that the materials or equipment identified are necessarily the best available for the purpose.

References

1. M. D. Eisaman, J. Fan, A. Migdall, and S. V. Polyakov, "Invited review article: Single-photon sources and detectors," Rev. Sci. Instrum. **82**, 071101 (2011).
2. F. Marsili, V. B. Verma, J. A. Stern, S. Harrington, A. E. Lita, T. Gerrits, I. Vayshenker, B. Baek, M. D. Shaw, R. P. Mirin, and S. W. Nam, "Detecting single infrared photons with 93% system efficiency," Nat. Photonics **7**, 210–214 (2013).
3. R. Lusche, A. Semenov, K. Ilin, M. Siegel, Y. Korneeva, A. Trifonov, A. Korneev, G. Goltsman, D. Vodolazov, and H.-W. Hübers, "Effect of the wire width on the intrinsic detection efficiency of superconducting-nanowire single-photon detectors," J. Appl. Phys. **116**, 043906 (2014).
4. L. Chen, D. Schwarzer, J. A. Lau, V. B. Verma, M. J. Stevens, F. Marsili, R. P. Mirin, S. W. Nam, and A. M. Wodtke, "Ultra-sensitive mid-infrared emission spectrometer with sub-ns temporal resolution," Opt. Express **26**, 14859–14868 (2018).
5. F. Marsili, F. Bellei, F. Najafi, A. E. Dane, E. A. Dauler, R. J. Molnar, and K. K. Berggren, "Efficient single photon detection from 500 nm to 5 μm wavelength," Nano Lett. **12**, 4799–4804 (2012).
6. L. Chen, D. Schwarzer, V. B. Verma, M. J. Stevens, F. Marsili, R. P. Mirin, S. W. Nam, and A. M. Wodtke, "Mid-infrared laser-induced fluorescence with nanosecond time resolution using a superconducting nanowire single-photon detector: New technology for molecular science," Accounts Chem. Res. **50**, 1400–1409 (2017).
7. C. M. Natarajan, M. G. Tanner, and R. H. Hadfield, "Superconducting nanowire single-photon detectors: physics and applications," Supercond. Sci. Technol. **25**, 063001 (2012).
8. T. Yamashita, S. Miki, W. Qiu, M. Fujiwara, M. Sasaki, and Z. Wang, "Temperature dependent performances of superconducting nanowire single-photon detectors in an ultralow-temperature region," Appl. Phys. Express **3**, 102502 (2010).
9. X. Yang, H. Li, W. Zhang, L. You, L. Zhang, X. Liu, Z. Wang, W. Peng, X. Xie, and M. Jiang, "Superconducting nanowire single photon detector with on-chip bandpass filter," Opt. Express **22**, 16267–16272 (2014).
10. K. Smirnov, Y. Vachtomin, A. Divochiy, A. Antipov, and G. Goltsman, "Dependence of dark count rates in superconducting single photon detectors on the filtering effect of standard single mode optical fibers," Appl. Phys. Express **8**, 022501 (2015).
11. H. Shibata, K. Shimizu, H. Takesue, and Y. Tokura, "Ultimate low system dark-count rate for superconducting nanowire single-photon detector," Opt. Lett. **40**, 3428–3431 (2015).
12. W. J. Zhang, X. Y. Yang, H. Li, L. X. You, C. L. Lv, L. Zhang, C. J. Zhang, X. Y. Liu, Z. Wang, and X. M. Xie, "Fiber-coupled superconducting nanowire single-photon detectors integrated with a bandpass filter on the fiber end-face," Supercond. Sci. Technol. **31**, 035012 (2018).
13. *Sectors & Applications: Case Studies—Gas Spectroscopy*, http://www.eblanaphotonics.com/sectors-and-applications.php.

OSA CONTINUUM

14. B. Jalali, "Nonlinear optics in the mid-infrared," Nat. Photonics **4**, 506–508 (2010).
15. D. Elvira, A. Michon, B. Fain, G. Patriarche, G. Beaudoin, I. Robert-Philip, Y. Vachtomin, A. V. Divochiy, K. V. Smirnov, G. N. Gol'tsman, I. Sagnes, and A. Beveratos, "Time-resolved spectroscopy of InAsP/InP(001) quantum dots emitting near 2 μm," Appl. Phys. Lett. **97**, 131907 (2010).
16. G. Tao, H. Ebendorff-Heidepriem, A. M. Stolyarov, S. Danto, J. V. Badding, Y. Fink, J. Ballato, and A. F. Abouraddy, "Infrared fibers," Adv. Opt. Photon. **7**, 379–458 (2015).
17. *Fused Silica / Fused Quartz*, https://escooptics.com/pages/materials-fused-silica-quartz.
18. H. Osanai, T. Shioda, T. Moriyama, S. Araki, M. Horiguchi, T. Izawa, and H. Takata, "Effect of dopants on transmission loss of low-OH-content optical fibres," Electron. Lett. **12**, 549–550 (1976).
19. R. Olshansky, "Propagation in glass optical waveguides," Rev. Mod. Phys. **51**, 341–367 (1979).
20. H. Murata and N. Inagaki, "Low-loss single-mode fiber development and splicing research in Japan," IEEE J. Quantum Electron. **17**, 835–849 (1981).
21. *Single Mode Fiber: 1.7 to 2.3 μm*, https://www.thorlabs.com/newgrouppage9.cfm?objectgroup_id=949.
22. *Corning SMF-28e+ Optical Fiber*, http://www.corning.com/media/worldwide/coc/documents/Fiber/PI1463_6-13.pdf.
23. M. Písařík, P. Peterka, S. Zvánovec, Y. Baravets, F. Todorov, I. Kašík, and P. Honzátko, "Fused fiber components for "eye-safe" spectral region around 2 μm," Opt. Quantum Electron. **46**, 603–611 (2014).
24. J. Ballato, H. Ebendorff-Heidepriem, J. Zhao, L. Petit, and J. Troles, "Glass and process development for the next generation of optical fibers: a review," Fibers **5** (2017).
25. D. Marcuse, "Curvature loss formula for optical fibers," J. Opt. Soc. Am. **66**, 216–220 (1976).
26. R. T. Schermer and J. H. Cole, "Improved bend loss formula verified for optical fiber by simulation and experiment," IEEE J. Quantum Electron. **43**, 899–909 (2007).
27. R. T. Schermer, "Mode scalability in bent optical fibers," Opt. Express **15**, 15674–15701 (2007).